Convergence of the augmented-space recursion

1997 J. Phys.: Condens. Matter 9 10701

(http://iopscience.iop.org/0953-8984/9/48/013)

J. Phys.: Condens. Matter **9** (1997) 10701–10714. Printed in the UK PII: S0953-8984(97)84430-X

Convergence of the augmented-space recursion

Subhradip Ghosh, Nityananda Das and A Mookerjee

S N Bose National Centre for Basic Sciences, JD Block, Sector 3, Salt Lake City, Calcutta 700091, India

Received 20 May 1997

Abstract. In this communication we study the convergence of the augmented-space recursion and illustrate the errors produced because of using only a finite part of the full augmented space and termination of the recursion after a finite number of steps. We illustrate this by using a TB-LMTO-based augmented-space formalism for a 50–50 AgPd alloy and studying how the moments of the density of states, the Fermi energy and the band energy converge

1. Introduction

In a series of recent communications [1–8] we have illustrated the applicability and usefulness of the augmented-space method in conjunction with the recursion technique of Haydock *et al* [9] in describing configuration-averaged properties of disordered alloys. These averages include correlated configuration fluctuations of clusters, which are not taken into account in the standard mean-field theories of alloys, and the calculations have been done using first-principles descriptions like the tight-binding linearized muffin-tin orbitals method (TB-LMTO). One of the remaining uncertainties of the method, in comparison with the usual k-space integration mean-field techniques, is how to demonstrate the convergence of the recursion in augmented space. In an earlier paper [3] we showed that the use of the local symmetries of the underlying lattice in real space and the symmetries of the augmented space arising out of the homogeneity of the disorder† allows us to carry out the recursion in an invariant subspace of the full augmented space. This subspace is of much reduced rank and therefore allows recursion to proceed to sufficient steps to ensure accuracy. Sanyal *et al* [6] showed that a transformation of the Hamiltonian allows us to treat the alloy system as if it were one with diagonal disorder alone. Ghosh *et al* [10] started from this transformed Hamiltonian and showed, by using recursions at different energies, that the continued-fraction coefficients have very weak energy dependence. They illustrated that by carrying out recursions at a few selected *seed* energies across the spectrum we may spline fit the coefficients across the spectral range and obtain the density of states accurately and within a very economical computational time. In this communication we shall use the above ideas and illustrate the nature of the convergence of various calculated physical quantities.

Since the details of the method have been described at length in the earlier articles [1–10], we shall introduce here only the essential results on which our calculations are based. The main basis of the method involves constructing the configuration space of the

† Homogeneity of the disorder requires the probability densities of the Hamiltonian matrix elements in real space to be independent of the site label.

0953-8984/97/4810701+14$19.50

Hamiltonian parameters. For a binary random distribution this space is isomorphic to the configuration space of an Ising model on the lattice. The augmented space is the product space of this configuration space and the lattice space spanned by the countable tight-binding LMTO basis. The augmented-space theorem then states that any physical quantity built out of the following Hamiltonian projected onto the so-called *average state* of the system (analogous to the spin-aligned state of the Ising model) is *exactly* the configuration average:

$$\tilde{\mathcal{H}} = \mathbf{H}_1\tilde{\mathbf{I}} + \mathbf{H}_2\sum_R \mathbf{P}_R \otimes \mathbf{P}^R_\downarrow + \mathbf{H}_3\sum_R \mathbf{P}_R \otimes \{\mathbf{T}^R_{\downarrow\uparrow} + \mathbf{T}^R_{\uparrow\downarrow}\} + \sum_R\sum_{R'} \mathbf{H}_4\mathbf{T}_{RR'} \otimes \mathbf{I} \tag{1}$$

where, for calculations of averaged local densities of states for a constituent labelled by λ, we have

$$\begin{aligned}
\mathbf{H}_1 &= A(\mathbf{C}/\boldsymbol{\Delta})\boldsymbol{\Delta}_\lambda - (EA(1/\boldsymbol{\Delta})\boldsymbol{\Delta}_\lambda - 1)\\
\mathbf{H}_2 &= B(\mathbf{C}/\boldsymbol{\Delta})\boldsymbol{\Delta}_\lambda - EB(1/\boldsymbol{\Delta})\boldsymbol{\Delta}_\lambda\\
\mathbf{H}_3 &= F(\mathbf{C}/\boldsymbol{\Delta})\boldsymbol{\Delta}_\lambda - EF(1/\boldsymbol{\Delta})\boldsymbol{\Delta}_\lambda\\
\mathbf{H}_4 &= (\boldsymbol{\Delta}_\lambda)^{-1/2}S_{RR'}(\boldsymbol{\Delta}_\lambda)^{-1/2}\\
A(Z) &= xZ_A + yZ_B\\
B(Z) &= (y-x)(Z_A - Z_B)\\
F(Z) &= \sqrt{xy}(Z_A - Z_B).
\end{aligned}$$

$\mathbf{C}$, $\boldsymbol{\Delta}$ and $\mathbf{S}$ are matrices in angular momenta, the first two being diagonal.

When we talk of convergence of the recursion method, we have to be careful to state precisely what we mean. Finite-space approximants to Green functions do not converge for real energy values. This problem arises in every computational method, as noted by Haydock [11]. The problem definitely arises in the usual k-space integration techniques, where methods using either complex energies or complex ks have been attempted. The cause of this non-convergence is that an arbitrary small perturbation, such as the adding of a single atom to a large but finite system, can shift all of the eigenvalues of the system. This causes an infinite change in the Green function near its corresponding poles. Thus, the precise meaning of the convergence of the recursion should imply the convergence of physical quantities built out of it. Most physical quantities are averages over the spectrum of the type

$$F(E) = \int_{-\infty}^{E} f(E')n(E')\,\mathrm{d}E'.$$

It is the convergence of these quantities which will decide whether the recursion is convergent or not. For example, the Fermi energy is defined by

$$\int_{-\infty}^{E_F} n(E')\,\mathrm{d}E' = n_e$$

where n_e is the total number of electrons, while the band energy is

$$U = \int_{-\infty}^{E_F} E'n(E')\,\mathrm{d}E'.$$

We shall study in general the convergence of indefinite integrals of the kind

$$M_k(E) = \int_{-\infty}^{E} (E')^k n(E')\,\mathrm{d}E'.$$

The integrand E'^k is monotonic and well behaved within the integration range.

Errors can arise in the recursion procedure from three distinct sources: (i) the error that arises because we carry out a finite number of recursion steps and then terminate the continued fraction using one of the available terminators; (ii) the error that arises because we choose a large but finite cluster in real space; and (iii) the error that arises because we choose a finite subspace of the configuration space. We shall examine all three sources systematically and make statements about our results.

2. Error analysis of the continued fraction

We shall first carry out a simple error analysis of the continued-fraction expression for the Green function, because of the errors created in the continued-fraction coefficients. The procedure is similar to the one discussed by Haydock [11].

The recursion is a two-term recurrence relation. We may therefore generate from this a pair of linearly independent sets of polynomials through the relations

$$b_{n+1}X_{n+1}(E) = (E - a_n)X_n(E) - b_nX_{n-1} \tag{2}$$

where X_n is either P_n or Q_n according to the initial conditions:

$$P_1(E) = 1 \qquad P_2(E) = (E - a_1)/b_2$$
$$Q_1(E) = 0 \qquad Q_2(E) = 1.$$

The approximated Green function in terms of the terminator $T(E)$ is given by

$$G_N(E) = \frac{Q_{N+1}(E) - b_N Q_N(E)T(E)}{b_1[P_{N+1}(E) - b_N P_N T(E)]}.$$

The terminator determines entirely the essential singularities of the spectrum. Haydock [11] showed that a finite composition of fractional linear transformations like the one above can at most add a finite number of poles to the spectrum. The essential singularities of the exact $G(E)$ and $T(E)$ coincide. The fractional linear transformation redistributes the spectral weights over the spectrum.

Let us now assume that we make errors $\{\delta a_n, \delta b_n\}$ in the corresponding continued-fraction coefficients. If we now start generating the orthogonal polynomials, starting from the exact initial conditions, but with the errors in the continued-fraction coefficients, we shall obtain a pair of sets $\{\tilde{P}_n\}$ and $\{\tilde{Q}_n\}$. In general we shall have

$$\tilde{P}_n(E) = (1 + A_n(E))P_n(E) + B_n(E)Q_n(E).$$

If we substitute this back into the recurrence relation and keep only the first-order terms in the errors,

$$\begin{aligned} A_n(E) &= \{\delta a_n\,[P_{n+1}(E)Q_{n+1}(E)] + \delta b_n\,[P_n(E)Q_{n+1}(E) + P_{n+1}(E)Q_n(E)]\}/b_1 \\ B_n(E) &= \{-\delta a_n\,P_{n+1}(E)^2 - \delta b_n\,[2P_n(E)P_{n+1}(E)]\}/b_1. \end{aligned} \tag{3}$$

Using the above and the expression for the local density of states, we find that the first-order relative error produced in the local density of states is

$$\frac{\delta n(E)}{n(E)} = -2\left[\left\{\sum_{n=1}^{\infty} A_n(E)\right\} + b_1 R(E)\left\{\sum_{n=0}^{\infty} B_n(E)\right\}\right]$$

where $R(E) = \mathcal{R}\,G(E)$. We define the weighted Hilbert transforms of $P_n(E)$ as the so-called associated functions:

$$\mathcal{Q}_n(E) = \mathcal{R}\left\{\int_{-\infty}^{\infty} \frac{P_n(E')n(E')}{E - E'}\,\mathrm{d}E'\right\}.$$

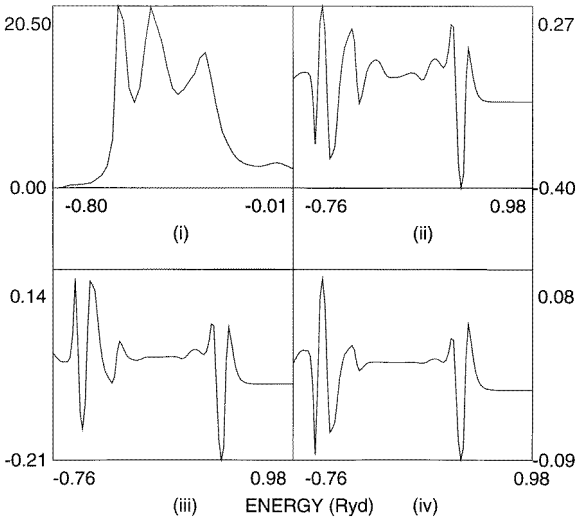

(a)

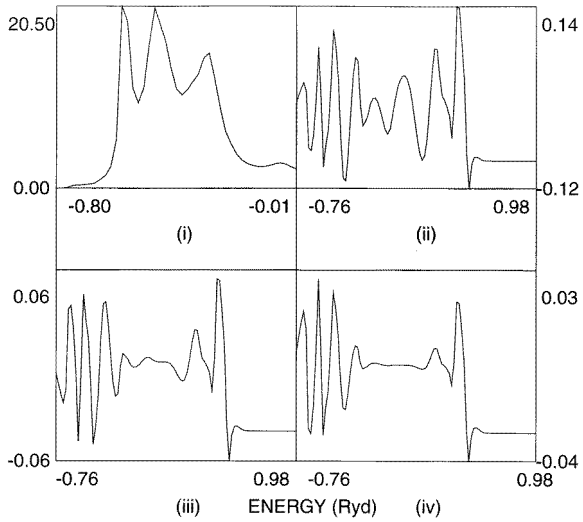

(b)

Figure 1. The moment difference functions for the 50–50 AgPd alloy, using seven augmented-space shells and termination after different numbers of recursions: (a) (i) $M_0^{8,4}$, (ii) $M_0^{8,5}$, (iii) $M_0^{8,6}$, (iv) $M_0^{8,7}$; (b) (i) $M_1^{8,4}$, (ii) $M_1^{8,5}$, (iii) $M_1^{8,6}$, (iv) $M_1^{8,7}$; (c) (i) $M_2^{8,4}$, (ii) $M_2^{8,5}$, (iii) $M_2^{8,6}$, (iv) $M_2^{8,7}$.

These associated functions are also solutions of the three-term recursion. They are not polynomials, but are nevertheless orthogonal to the set $P_n(E)$.

In terms of these, the error in the density of states is

$$\frac{\delta n(E)}{n(E)} = \frac{2}{b_1}\left\{\sum_{n=1}^{\infty}\left[\delta a_n\, P_{n+1}(E)\mathcal{Q}_{n+1}(E) + 2\,\delta b_{n+1}\, P_{n+1}\mathcal{Q}_{n+2}\right]\right\}. \tag{4}$$

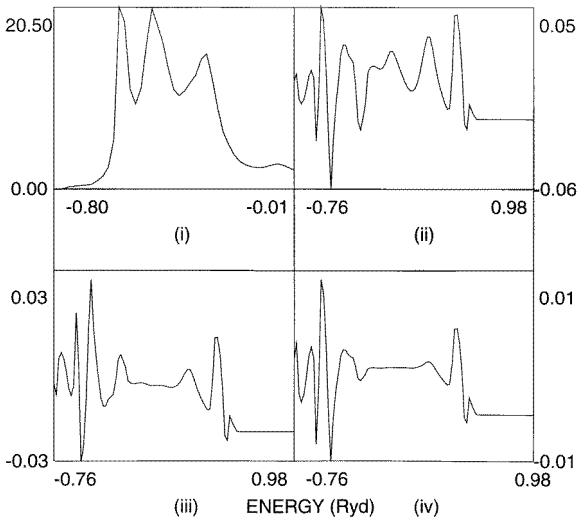

(c)

Figure 1. (Continued)

Such an expression is familiar from the multiple-scattering t-matrix approaches. The above is actually the contribution of the *single-site t-matrix* for a set of scatterers at the *sites* labelled by n, formed from the sum of individual single-site scatterers. This approximation is rather similar to that which forms the basis of the multiple-scattering approach to the coherent potential approximation.

The error in the Fermi energy will be given by

$$\delta E_F = -\frac{1}{n(E_F)} \sum_{n=1}^{\infty} \left\{ \delta a_n \, A_n^{(0)}(E_F) + \delta b_{n+1} \, B_n^{(0)}(E_F) \right\} \tag{5}$$

while the errors in the various moment functions are

$$\delta M_k(E) = \delta E_F \, E_F^k n(E_F) + \sum_{n=1}^{\infty} \left\{ \delta a_n \, A_n^{(k)}(E_F) + \delta b_{n+1} \, B_n^{(k)}(E_F) \right\} \tag{6}$$

where

$$\begin{aligned} A_n^{(k)}(E) &= \frac{2}{b_1} \int_{-\infty}^{E} P_{n+1}(E') \mathcal{Q}_{n+1}(E') (E')^k n(E') \, \mathrm{d}E' \\ B_n^{(k)}(E) &= \frac{4}{b_1} \int_{-\infty}^{E} P_{n+1}(E') \mathcal{Q}_{n+1}(E') (E')^k n(E') \, \mathrm{d}E'. \end{aligned} \tag{7}$$

2.1. Termination error

In all computational calculations, the recursion can be carried out at most to a finite number of steps, after which the continued fraction is terminated by a terminator function $T(E)$ as discussed earlier. We have used the terminator of Luchini and Nex which smoothly joins onto the rest of the continued fraction and which reproduces the band widths, the band weights and the essential singularities of the Green function at the band edges. Its spectral distribution is smooth, akin to a simple semicircular distribution.

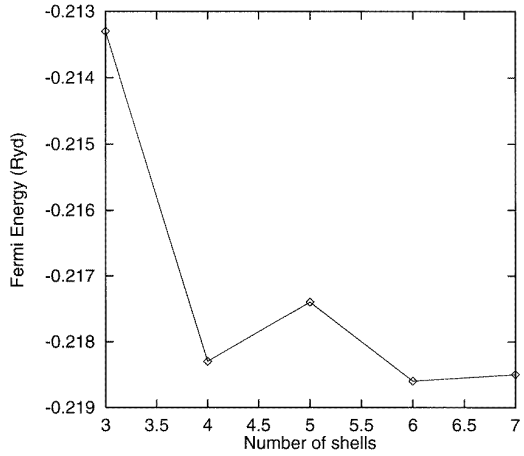

(a)

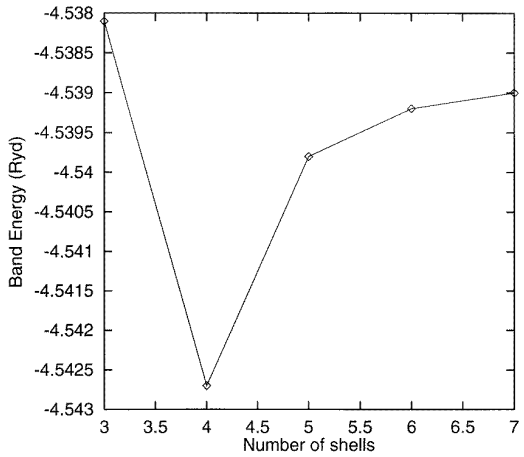

(b)

Figure 2. The convergence of the (a) Fermi energy and (b) band energy of a 50–50 AgPd alloy, using the first-order TB-LMTO Hamiltonian, as we terminate the continued fraction after different numbers of recursions on a seven-shell augmented-space cluster.

Consider two situations: one in which we terminate at the Nth step, and hence for which all coefficients for $n \leqslant N$ are free from the termination error; and another in which we terminate after $N+r$ steps. The recursive error in the Fermi energy and the band energy are

$$\Delta E_F^{N+r,N} = -\frac{1}{n(E_F)} \sum_{n=N+1}^{N+r+1} (\delta a_n \, A_n^{(0)} + \delta b_{n+1} \, B_n^{(0)})$$

$$\Delta U^{N+r,N} = \sum_{n=N+1}^{N+r+1} \left\{ \delta a_n \, (A_n^{(1)} - E_F A_n^{(0)}) + \delta b_{n+1} \, (A_n^{(1)} - E_F A_n^{(0)}) \right\}.$$

Here, $\Delta U^{N+r,N}$ is $\delta U^{N+r} - \delta U^N$ and δa_n and δb_{n+1} are the errors produced in these coefficients because of the termination where we replace the exact coefficients by the

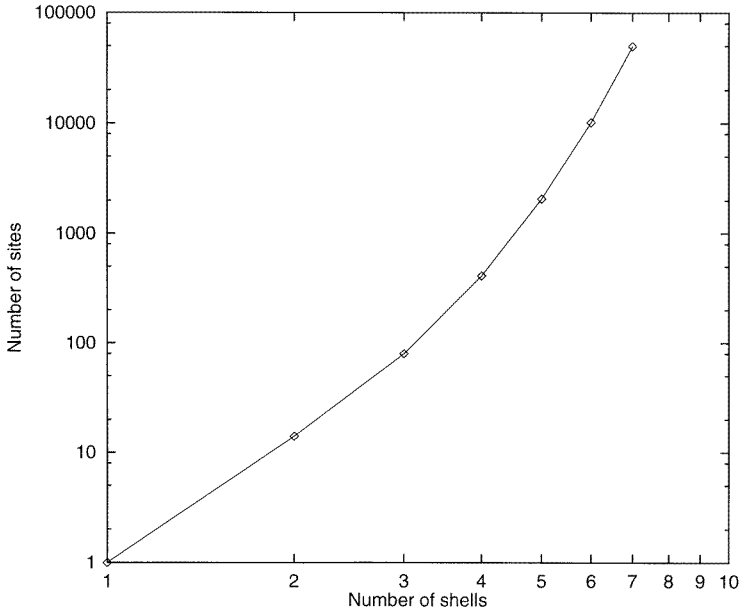

Figure 3. A log–log plot of the number of sites as we increase the number of shells in augmented space.

terminator coefficients. If the coefficients converge, then if N is sufficiently large these recursive errors also converge. This is consistent with Haydock's criterion of the divergence of the series $\sum(1/b_n)$.

To illustrate our results we have carried out the augmented-space recursion on a first-order TB-LMTO Hamiltonian for the 50–50 AgPd alloy. The calculation was done using the full LDA self-consistency program set up by us, including the symmetry and seed energy recursions described earlier. In figures 1(a)–1(c) we show the moment difference functions (a) for the zeroth moment, (b) for the first moment and (c) for the second moment. The differences are between terminations after (i) eight and four recursions, (ii) eight and five recursions, (iii) eight and six recursions and (iv) eight and seven recursions. These differences are shown across the entire energy range, including the positive-energy unoccupied states. The underlying augmented-space subspace on which the recursion is carried out was seven shells wide, starting from an initial site.

We can make the following statements.

(i) Termination after four or five recursions gives extremely inaccurate results. The range of the errors over the entire spectrum decreases quite rapidly as we terminate after more steps.

(ii) The range of errors also decreases as we look at higher moments. This seems to be a general observation—that the higher moments converge much faster than the lower ones.

Perhaps a much better illustration is shown in figures 2(a) and 2(b). This shows the behaviour of the Fermi energy and band energy as functions of the number of recursions before termination. Again we see that three or four recursions give very inaccurate results. However, these physical properties converge reasonably quickly when we go up to eight recursion steps. Further recursions reduce the errors to within the range of errors produced

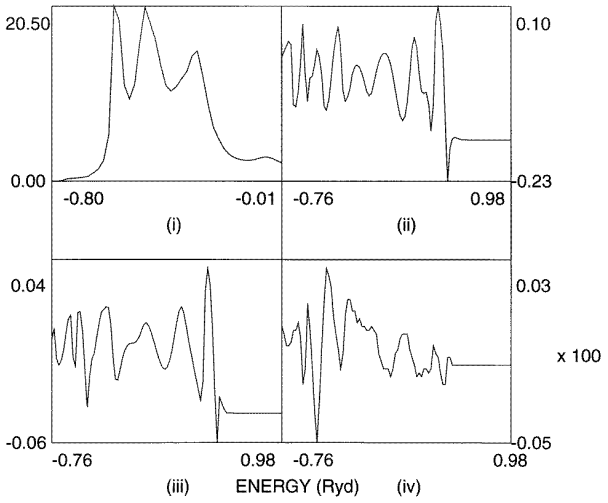

(a)

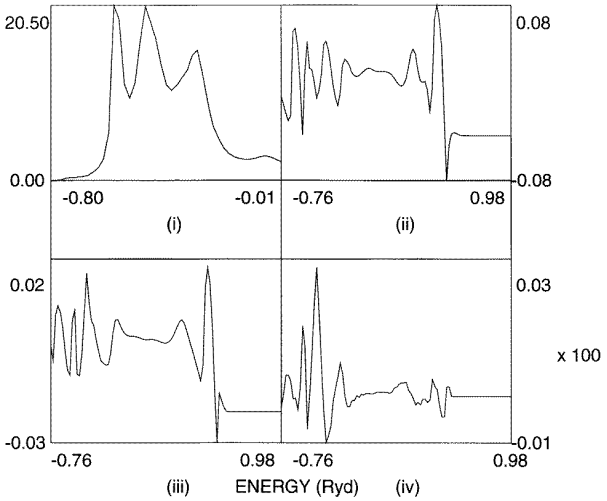

(b)

Figure 4. The moment difference functions for the 50–50 AgPd alloy, using six augmented-space shells but restricting the size of the underlying real-space cluster to different numbers of shells: (a) (i) the density of states, (ii) $M_0^{6,3}$, (iii) $M_0^{6,4}$, (iv) $M_0^{6,5}$; (b) (i) the density of states, (ii) $M_1^{6,3}$, (iii) $M_1^{6,4}$, (iv) $M_1^{6,5}$.

by the approximations within the TB-LMTO itself. So, as long as we are within the ambit of the first-order TB-LMTO basis, it is unfruitful to carry out recursions beyond this stage.

2.2. Finite-size errors

The termination error is not always the predominant error in recursion calculations. Starting from a single *state* $|\underline{R_i}, L, \{\emptyset\}\rangle$, the total number of *states* over which the subsequent recursively calculated basis spreads out, i.e. the rank of the subspace accessed by recursion,

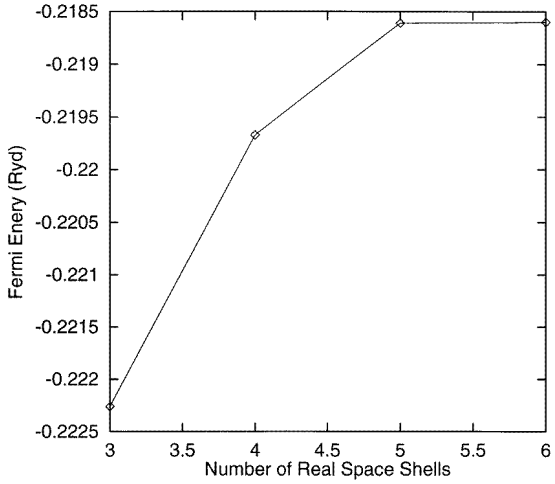

(a)

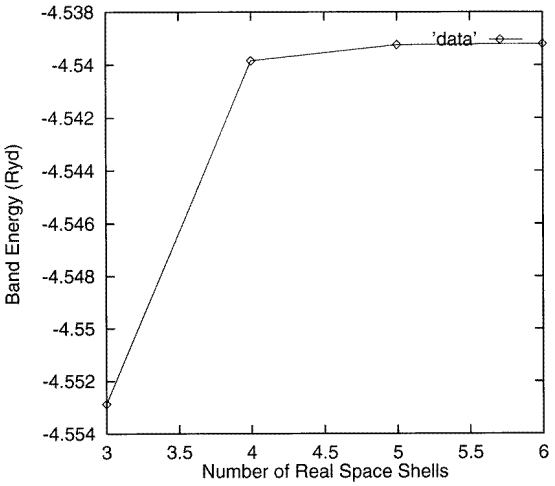

(b)

Figure 5. The convergence of the (a) Fermi energy and (b) band energy of a 50–50 AgPd alloy, using the first-order TB-LMTO Hamiltonian, as we carry out recursion on increasing sizes of the real-space cluster.

soon becomes prohibitively large. This is particularly true in the full augmented space. Not only are the lattice neighbours of the initial site accessed, but so also are all possible configurations of this cluster of sites. Figure 3 gives us some idea of the rank of the subspace accessed per recursion step of a binary alloy on a f.c.c. lattice. Since, for transition metals, there are nine orbitals per site, the total rank of the subspace accessed is actually nine times as large. It is this point which made some earlier workers on the augmented-space formalism state that it was a mathematically fascinating formalism, but computationally impractical [12]. However, in subsequent studies we showed [3–5] that the point group symmetries of the underlying lattice, the symmetry of the starting state and the underlying symmetries of the configuration space (in the case where the disorder is homogeneous) drastically reduce

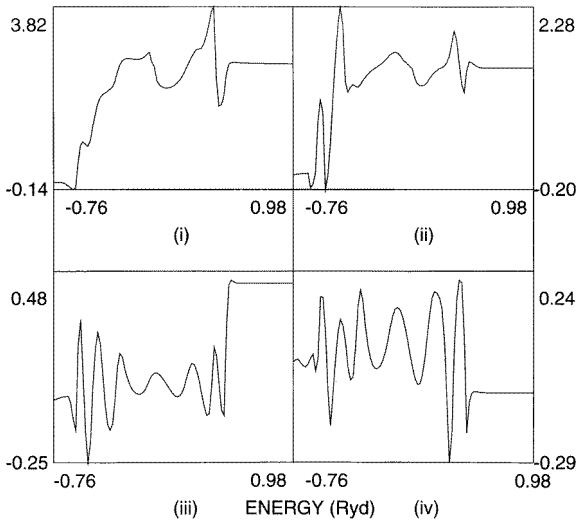

(a)

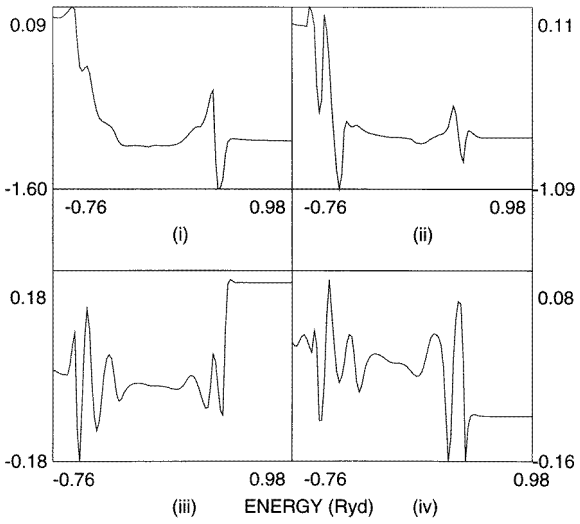

(b)

Figure 6. The moment difference functions for the 50–50 AgPd alloy, using different-sized augmented-space shells: (a) (i) the density of states, (ii) $M_0^{6,3}$, (iii) $M_1^{6,3}$, (iv) $M_2^{6,3}$; (b) (i) the density of states, (ii) $M_0^{6,4}$, (iii) $M_1^{6,4}$, (iv) $M_2^{6,4}$; (c) (i) the density of states, (ii) $M_0^{6,5}$, (iii) $M_1^{6,5}$, (iv) $M_2^{6,5}$.

the rank of the invariant subspace on which the recursion effectively acts.

Even after the reduction of the rank using local symmetries, we shall argue that we may in fact restrict our subspace to a given rank and carry out the recursion over a much larger number of steps. In this section, we shall analyse the error made when the recursion hits a subspace boundary and carries on further. Since we do not allow Hamiltonian elements within and outside this subspace, the problem is that of a perfectly reflecting boundary.

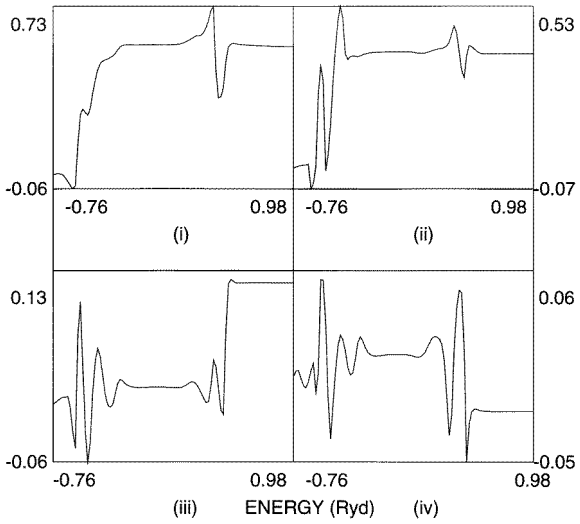

(c)

Figure 6. (Continued)

The continued-fraction coefficients can be expressed in terms of either of the Hänkel determinants of the Hamiltonian moments:

$$a_{n+1} = \frac{K_{n-2}}{K_{n-1}}\frac{H_n}{H_{n-1}} + \frac{K_n}{K_{n-1}}\frac{H_{n-1}}{H_n} \qquad n \geqslant 1$$

and

$$b_{n+1}^2 = \frac{H_n H_{n-2}}{H_{n-1}^2} \qquad n \geqslant 1$$

where

$$H_n = \begin{vmatrix} \mu_0 & \mu_1 & \dots & \mu_n \\ \mu_1 & \mu_2 & \dots & \mu_{n+1} \\ \dots & \dots & \dots & \dots \\ \mu_n & \mu_{n+1} & \dots & \mu_{2n} \end{vmatrix}$$

$$K_n = \begin{vmatrix} \mu_1 & \mu_2 & \dots & \mu_{n+1} \\ \mu_2 & \mu_3 & \dots & \mu_{n+2} \\ \dots & \dots & \dots & \dots \\ \mu_{n+1} & \mu_{n+2} & \dots & \mu_{2n+1} \end{vmatrix}.$$

Thus if we make sure that the rank of the accessed subspace is sufficiently large that its boundary is not hit by recursion up to M steps, then up to $2M$ moments of the density of states are exactly reproduced, and errors occur only from moment $2M+1$. For the coherent potential approximation for diagonal disorder, we know that the first eight moments are exact and the subsequent moments are $O((1/Z)^n)$, Z being the connectivity of the lattice. To obtain comparatively accurate results with recursion we must perform at least four steps of recursion and make sure that our estimates of errors in the subsequent recursion coefficients and the terminator are comparable with those of the CPA.

The question that we wish to ask is the following: if instead of stopping the recursion after M steps and completing it with a terminator we carry on recursions for further steps,

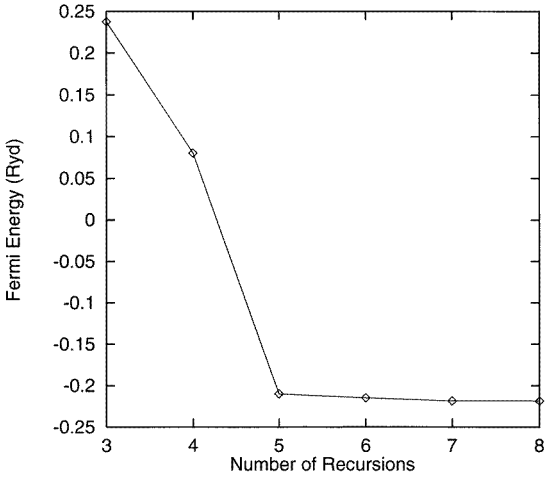

(a)

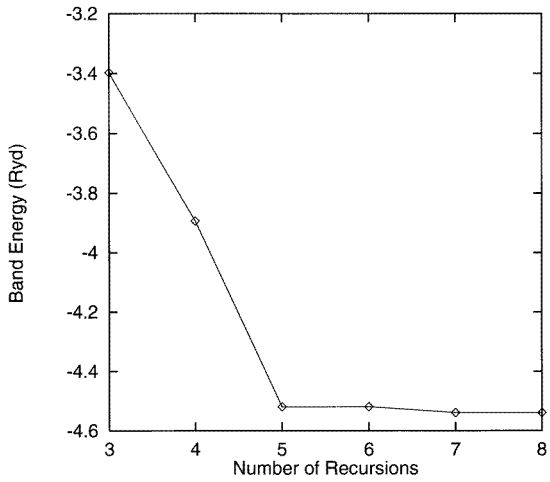

(b)

Figure 7. The convergence of the (a) Fermi energy and (b) band energy of a 50–50 AgPd alloy, using the first-order TB-LMTO Hamiltonian, as we carry out recursion on increasing sizes of the augmented-space cluster.

do we make unacceptable errors in the subsequent moments? Let us first illustrate what we obtain from our numerical work on AgPd. We have constructed a six-shell augmented-space map, but terminated its real-space part after three, four and five shells on a f.c.c. lattice. In taking the augmented-space shells further out, we have made sure that all of the configuration fluctuations are taken into account. The approximation is that the rank of the underlying real-space lattice is taken to be finite. In all cases nine steps of recursion were performed exactly and the procedure was terminated thereafter.

Figures 4(a) and 4(b) show the moment difference functions for the (a) first moment and (b) second moment for differences between (i) six and three real-space shells, (ii) six and four real-space shells, and (iii) six and five real-space shells. Figures 5(a) and 5(b)

show the convergence of the Fermi and band energies with increasing number of real-space shells. Our observations are similar to those for the termination errors. The error range across the spectrum decreases rapidly as we increase the number of real-space shells. By the time that we have reached six shells from the starting point the errors in the physical quantities are within the range of errors in the basic formulation. Higher moments tend to converge faster.

Do we understand why this is so? Perhaps the best way to illustrate this is to go from the moment description of the continued-fraction coefficients to a graphical language in terms of closed paths on the underlying lattice. We construct these paths by assigning to each member of the countable basis a *vertex* and to each off-diagonal matrix element of the Hamiltonian a *link*. A sequence of connected vertices and links forms a *path*. Moments can be written as sums of contributions of paths starting and ending at the initial site from which the recursion begins. Such a *geometric* interpretation has been used earlier [13–15]. In the language of paths, if we restrict our real-space lattice to a finite number of shells, then the contributions of paths which cross this shell are neglected. However, if we look at the set of closed paths of a certain length N, when N is large, the number of paths which wind round the initial site without hitting the boundary by far dominates the paths that spread outwards crossing it. This is certainly true when the coordination of the lattice is large and the paths have greater freedom for twisting around. It is not surprising that if we take our underlying lattice to sufficiently large shells outwards, the errors made in discounting paths crossing the boundary may not be large, since most of the contributions of the coefficients will come from the winding paths which stay well within the boundary. Thus if we carry on our recursion even after the boundary has been hit, and subsequently too, the recursions will mostly sample the subspace inside the boundary.

Finally, we look at what happens when we restrict the entire augmented space itself to a finite shell. We should notice here that if we restrict the augmented space to within three shells, say, then automatically the real-space part is also restricted to within three shells. This is because the nth augmented-space shell is reached from the starting site by n operations of the effective Hamiltonian. Again in all cases nine recursions were carried out and the terminator attached thereafter.

In figures 6(a)–6(c) we show the moment differences for the zeroth to the second moments ((ii)–(iv)) for the difference between (a) six and three, (b) six and four and (c) six and five augmented-space shells. Figures 7(a) and 7(b) show the convergences of the Fermi and band energies. We notice that although the nature of the convergence is different from the monotonic one that we met earlier, by the time we reach seven shells in the augmented space the errors are well within the intrinsic errors of the TB-LMTO approximations themselves.

These systematic studies give us an indication that such convergence analysis is essential for every case under study using the augmented-space recursions. Errors will vary from system to system. The most significant error comes from truncation of the real-space lattice. Truncation in configuration space becomes significant only when there is clustering-based or local-ordering-based structure in the density of states. Most of the time spent in carrying out the recursion elapses because of the large rank of the subspace in augmented space in which we carry out the recursion exactly. Termination errors are less significant and choice of good terminators often pays rich dividends as regards accuracy. In general, we may expect that nine to ten recursions on about seven augmented-space shells should provide us with the requisite error range of tolerance consistent with the errors in the basis of the representation (the TB-LMTO approximation in this case). However, for example, in the case of the impurity band of Cu in Zn, where one expects cluster-based structures in

the density of states, we may have to go as far as 14–15 steps of recursions on 9–10 augmented-space shells. This was reported earlier [7]. It should be noted that an advantage of disordered systems is that the density of states has far less structure than it has in ordered translationally invariant systems. The consequent convergence of the recursions is faster since the moments themselves fluctuate less for such smoother functions.

Acknowledgment

One of us (ND) would like to thank the Council of Scientific and Industrial Research, India, for providing me with financial assistance during the course of this work.

References

[1] Mookerjee A 1973 *J. Phys. C: Solid State Phys.* **6** 1340
[2] Datta A and Mookerjee A 1992 *Int. J. Mod. Phys.* B **6** 3295
[3] Saha T, Dasgupta I and Mookerjee A 1994 *J. Phys.: Condens. Matter* **6** L245
[4] Mookerjee A and Prasad R 1993 *Phys. Rev.* B **48** 17 724
[5] Dasgupta I, Saha T and Mookerjee A 1995 *Phys. Rev.* B **51** 3413
[6] Sanyal B, Biswas P P, Fakhruddin M, Halder A, Ahmed M and Mookerjee A 1995 *J. Phys.: Condens. Matter* **7** 8569
[7] Saha T and Mookerjee A 1997 *J. Phys.: Condens. Matter* **10** 2179
[8] Dasgupta I, Saha T, Mookerjee A and Das G P 1997 *J. Phys.: Condens. Matter* at press
[9] Haydock R, Heine V and Kelly M J 1975 *J. Phys. C: Solid State Phys.* **8** 2591
[10] Ghosh S, Das N and Mookerjee A 1997 *Indian J. Phys.* at press
[11] Haydock R 1982 *Solid State Physics* vol 35 (New York: Academic) p 257
[12] Kaplan T, Leath P L, Gray L J and Diehl H W 1980 *Phys. Rev.* B **21** 4230
[13] Haydock R 1972 *PhD Thesis* University of Cambridge
[14] Haydock R 1974 *J. Phys. A: Math. Gen.* **7** 2120
[15] Kumar V, Mookerjee A and Srivastava V K 1982 *J. Phys. C: Solid State Phys.* **15** 1939